Eidgenössische Technische Hochschule Zürich
Swiss Federal Institute of Technology Zurich

Evasion Problem

Determining the Existence of Evasion Paths in Mobile Sensor Networks

Julia Sollberger

Bachelor's Thesis

Bachelor's Degree Programme Mathematics
Department of Mathematics
Swiss Federal Institute of Technology (ETH) Zurich

Supervision

Dr. Sara Kališnik Hintz

July 14, 2023

Abstract

Imagine a mobile sensor network as a finite number of sensors moving around in a bounded domain. Each sensor surveys the area within a certain radius around itself, and two sensors can detect whether their observed, ball-shaped areas overlap. We would like to know if an evasion path exists, that is, if an intruder can move around in such a way that he remains undetected by the sensors. In *Evasion paths in mobile sensor networks*, Henry Adams and Gunnar Carlsson fall back on the work of Vin de Silva and Robert Ghrist, showing that while the time-varying connectivity data gives necessary conditions for the existence of an evasion path, it is not sufficient to fully determine in which cases an evasion path does or does not exist. In the two dimensional case, and by adding the sensor capabilities of measuring weak rotation and distances, Adams and Carlsson provide a way to fully determine the existence of an evasion path. This bachelor's thesis summarizes their results and provides additional background information.

Contents

1 Introduction

Consider an area surveilled by mobile sensors, where each sensor can observe the area within a fixed radius of its position. As the sensors move around, the covered and uncovered areas change. An intruder may want to avoid being detected by the sensors. They thus try to move around in such a way that they stay in the uncovered area at each point in time. Given the movements of the sensors, we would like to determine whether there is what we will call an "evasion path": a path the intruder can follow to evade the sensors. The problem of answering this question is what we will call the "evasion problem".

Of course, if at some point in time, the sensors cover the entire area, then the intruder has no possibility to evade the sensors. If, on the other hand, the uncovered area is non-empty at each point in time, the situation proves more interesting. Consider the following example:

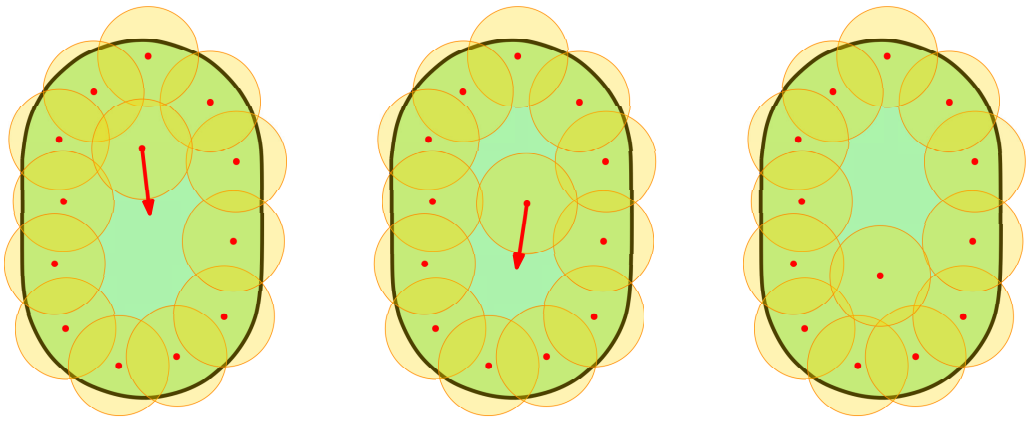

(a) (b) (c)

Figure 1: A sensor network at three different points in time. All sensors are static, except for one in the center that moves from top to bottom.

Even though the sensors never cover the entire area, it is not possible for an intruder to evade the sensors. Consider an intruder who, at the beginning in (a), is located in the uncovered area south of the moving sensor. They have no way to move past that sensor to get to the uncovered area north of the moving sensor in (c). No matter their movements, they will eventually be detected by the sensors. Thus, in this example, no evasion path exists.

In the special case where all the sensors are static, the problem turns into a question of coverage. We denote the union of all sensor balls, that is, the area surveyed by the sensors, by K. For a d-dimensional domain, it turns out that the entire domain is covered by the sensor balls if and only if $\dim H^{d-1}(K) = 0$, where we take homology groups with coefficients in a field. The result follows from Alexander Duality, which gives isomorphisms in homology between a space in $\mathbb{R}^n$ and its complement.

For mobile sensor networks we consider the covered area X in "spacetime" $\mathcal{D} \times [0,1]$. A reformulated theorem from de Silva and Ghrist [7] gives a necessary condition for the existence of an evasion path:

Theorem. *An evasion path can only exist if there does not exist an* $[\alpha]$ *in* $H_d(X, \partial\mathcal{D} \times [0,1])$ *such that* $0 \neq [\partial\alpha] \in H_{d-1}(\partial\mathcal{D} \times [0,1])$.

Consider for example the spacetime of the sensor network in Figure 2.

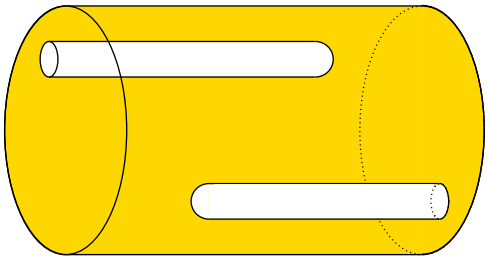

Figure 2: Spacetime of an example mobile sensor network with a 2-dimensional disc as the domain. The time coordinate is illustrated along the horizontal axis, and the orange area represents the covered region.

One can imagine a cycle representative α that satisfies the condition in the theorem to be a membrane, spanning vertically across the entire domain in spacetime and thereby separating the two connected uncovered areas (white). Intuitively, it is then clear that an intruder, starting from the first uncovered region that connects to time 0, cannot reach the second uncovered region that connects to time 1.

To apply this result, one would need to know the positions of the sensors. By modeling the covered area with simplicial complexes, another version of this result that relies only on the time-varying connectivity data is obtained.

A second necessary condition for the existence of an evasion path is given by constructing levelset zigzag diagrams from the covered area in spacetime and applying zigzag persistence homology. As we will see, it is impossible, given only the time-varying connectivity data, to fully determine whether or not an evasion path exists.

This thesis follows closely the work of Henry Adams and Gunnar Carlsson [1], who approach the problem by looking at the time-varying Čech complex of the sensor balls. Necessary background theory on simplicial complexes, Alexander Duality, fibrewise spaces and zigzag homology is covered in Section 2. Using the introduced terminology, we will be able to formalize the evasion problem in Section 3 and treat the special case of a static sensor network. Finally, Section 4 approaches the evasion problem by introducing stacked Čech complexes and zigzag homology. Subsection 4.3 elaborates on the insufficiency of the time-varying connectivity data. Last but not least, Subsection 4.4 gives a constructive solution to the evasion problem in the two dimensional case with added sensor capabilities, and working with time-varying alpha complexes instead of Čech complexes.

2 Background

This section provides background information that is needed in the subsequent sections, covering simplicial complexes, Alexander Duality, fibrewise spaces and zigzag persistence.

2.1 Simplicial Complexes

We start by introducing simplicial complexes, including two constructions of simplicial complexes, namely Čech complexes and alpha complexes. This subsection follows Carlsson [3] and Hatcher [10].

Definition. *Let $V = \{v_0, ..., v_n\}$ be a subset of $n+1$ points of $\mathbb{R}^d$ such that the n difference vectors $v_1 - v_0, ..., v_n - v_0$ are linearly independent. Then, the $n-$**simplex spanned by** V is the convex hull $\sigma(V)$ of V in $\mathbb{R}^d$. A **face** of a simplex $\sigma = \sigma(V)$ is a simplex $\sigma(T)$ spanned by any non-empty subset $T \subset V$.*

Definition. *A (finite) **simplicial complex** is a finite collection $\mathcal{X}$ of simplices in Euclidean space such that:*

(1) Given any simplex σ in $\mathcal{X}$, all its faces are also in $\mathcal{X}$.

(2) The intersection $\sigma \cap \tau$ of any two simplices σ and τ in $\mathcal{X}$ is a face of both σ and τ. By (1) it follows that $\sigma \cap \tau$ is also in $\mathcal{X}$.

Example 1. The following figure depicts a simplicial complex embedded in $\mathbb{R}^3$ that consists of nine 0-simplicies = points, fifteen 1-simplices, nine 2-simplices and one 3-simplex:

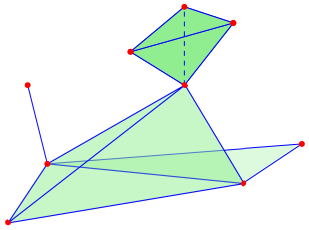

Figure 3: An example of a simplicial complex.

Definition. *An **abstract simplicial complex** is a pair*

$$X = (V(X), \Sigma(X)),$$

where $V(X)$ *is some finite set – the **vertices**,*

and $\Sigma(X) \subset \mathcal{P}(V(X)) \setminus \varnothing$ *– the **simplices** – such that* $\left.\begin{matrix}\sigma \in \Sigma(X) \\ \varnothing \neq \tau \subset \sigma\end{matrix}\right\} \implies \tau \in \Sigma(X).$

There is the following relation between (geometric) simplicial complexes and abstract simplicial complexes:

Every simplicial complex gives an abstract simplicial complex by taking $V(X)$ to be the set of all vertices that appear in $\mathcal{X}$ and $\Sigma(X)$ to be the collection of all sets $S \subset V(X)$ such that $\sigma(S)$ is a simplex in $\mathcal{X}$.

On the other hand, we can retreive from every abstract simplicial complex a simplicial complex by taking its *geometric realization*. That is, if $V(X)$ consists of n vertices, a subcomplex of the standard $(n-1)$-dimensional simplex Δ^{n-1}. Each element in $V(X)$ is assigned bijectively to one of the n vertices $(0, ..., 1, ..., 0)$ of Δ^{n-1}, and a face $[e_{i_1}, ..., e_{i_k}]$ of Δ^{n-1} is included in the geometric realization exactly when the points in $V(X)$ assigned to $e_{i_1}, ..., e_{i_k}$ form a simplex in $\Sigma(X)$ as well. It is easy to check that this construction satisfies the definition of a simplicial complex.

Every two simplicial complexes that give the same abstract simplicial complex are homeomorphic to each other.

Example 2. Consider the following simplicial complex embedded in $\mathbb{R}^2$:

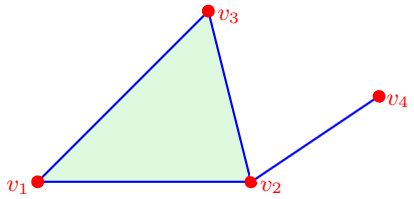

By applying the procedure described above, we get the following abstract simplicial complex:

$$\rightsquigarrow \begin{cases} V = \{v_1, v_2, v_3, v_4\} \\ \Sigma = \big\{\{v_1\}, \{v_2\}, \{v_3\}, \{v_4\}, \{v_1, v_2\}, \{v_1, v_3\}, \{v_2, v_3\}, \{v_2, v_4\}, \{v_1, v_2, v_3\}\big\}. \end{cases}$$

We could now in turn take the geometric realization of this abstract simplicial complex, yielding a simplicial complex embedded in $\mathbb{R}^4$ that is homomorphic to the original simplical complex.

Čech Complexes and Alpha Complexes

This subsection follows [8].

Definition. *Let $\mathcal{U} = \{U_\alpha\}_{\alpha \in A}$ be a collection of sets. The **nerve** of the collection $\mathcal{U}$ is the (abstract) simplicial complex $N(\mathcal{U})$ defined as follows:*

vertex set V = index set A

simplices $\sigma = \{\alpha_0, ..., \alpha_k\} \in \Sigma$ for all $\{\alpha_0, ..., \alpha_k\} \subset A$ such that $U_{\alpha_0} \cap U_{\alpha_1} \cap ... \cap U_{\alpha_k} \neq \varnothing$.

Let us quickly check that this definition satisfies the conditions of an abstract simplicial complex: Take any $\sigma = \{\alpha_0, ..., \alpha_k\} \in \Sigma$. Then $U_{\alpha_0} \cap ... \cap U_{\alpha_k}$ is non-empty, so for all non-empty subsets $\tau = \{\alpha_{i_0}, ..., \alpha_{i_l}\}$ of σ, $U_{\alpha_{i_0}} \cap ... \cap U_{\alpha_{i_l}}$ is also non-empty. Thus $\tau \in \Sigma$ for all non-empty $\tau \subset \sigma$.

Example 3. Consider the five subsets of the plane in Figure 4. The nerve of these subsets is the abstract simplicial complex consisting of

- five 0-simplices, one for each subset,
- six 1-simplices, one for each unordered pair of subsets whose intersection is non-empty, and
- one 2-simplex for the three subsets whose intersection is non-empty.

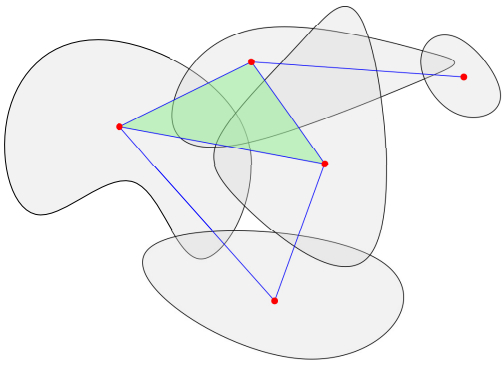

Figure 4: The simplicial complex depicted is the nerve complex of the example covering consisting of the five grey subsets.

The simplicial complex illustrated in Figure 4 is homeomorphic to the geometric realization of the nerve. Illustrating the nerve in two dimensions is only possible, since there are no simplices of dimension 3 or higher in this example.

An easy way to use the construction of the nerve to create a simplicial complex from a (partial) cover of a metric space is the Čech complex.

Definition. *Let (M, d) be a metric space; $P = \{p_1, ..., p_n\} \subset M$ a finite subset and $r \in (0, \infty)$. The* ***Čech complex*** *$C_r(P)$ is the nerve of the set of closed balls $\{B_{p_i}(r)\}_{i=1}^n$.*

Example 4. Consider four points in the plane equipped with Euclidean metric. For increasing radii, more and more simplicies are a part of the Čech complex (see Figure 5). Once all four balls $B_{p_i}(r)$ intersect, the Čech complex is a 3-simplex with all its faces included, and therefore can no longer be realized in the plane.

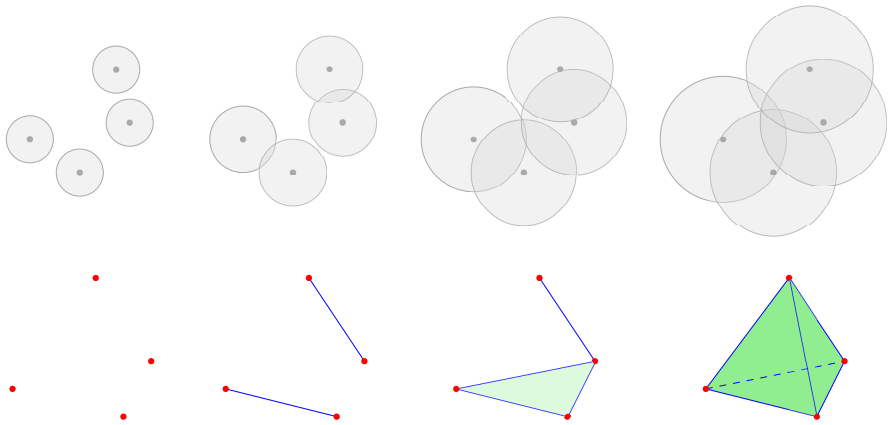

Figure 5: Balls around the four points and the resulting (geometric realizations of the) Čech complexes at different radii r.

An important property of nerves that we will apply to certain Čech complexes later on in the thesis is the *Nerve Theorem* that first appeared in the works of Leray [12] and Borsuk [2]:

Theorem 1 (Nerve Theorem)**.** *Let $\mathcal{U}$ be a finite cover of a metric space M. Suppose that every non-empty intersection of elements in $\mathcal{U}$ is contractible. Then, the underlying space $|N(\mathcal{U})|$, that is the geometric realization of the nerve $N(\mathcal{U})$, is homotopy equivalent to M.*

When r, relative to the distances between the distances of points in P, is large, the Čech complex $C_r(P)$ becomes very big. In the following we construct a subcomplex of $C_r(P)$, the so-called *alpha complex* that we will use in Section 4.4. Since that subsection treats only the special case where the sensor network is embedded in a plane, we will introduce alpha complexes only in $\mathbb{R}^2$. The definition uses the construction of *Voronoi cells*:

Definition. *Given a finite subset of points $P \subset \mathbb{R}^2$, we define the* ***Voronoi cells***

$$V_p := \{x \in \mathbb{R}^2 : d(x, p) \leq d(x, q) \ \ \forall q \in P\}.$$

Voronoi cells are constructed by taking perpendicular bisectors of sections between points. An example is illustrated in Figure 6.

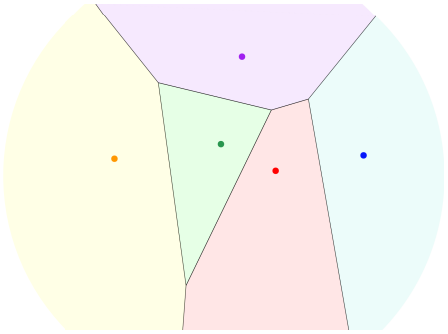

Figure 6: Voronoi cells for five points in the plane.

Definition. *Let $r \in [0, \infty)$. Given a finite set P of points in $\mathbb{R}^2$, define* ***alpha cells***

$$R_p(r) := V_p \cap B_p(r),$$

where V_p is the Voronoi cell of p in P. The ***alpha complex*** *at r is the nerve of $\{R_p(r)\}_{p \in P}$.*

Since the Čech complex is the nerve of $\{B_p(r)\}_{p \in P}$, and since $R_p(r) \subset B_p(r)$ for all r and p, it is clear that the alpha complex is a subcomplex of the Čech complex. See Figure 7 for an example.

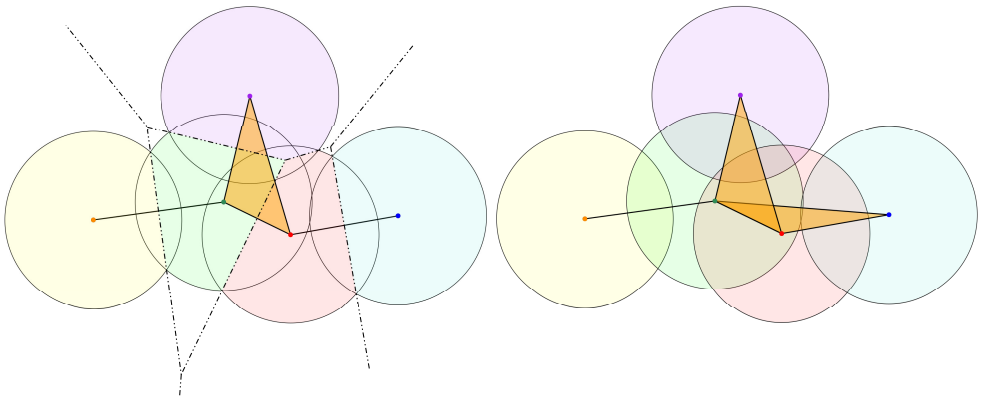

(a) Alpha Complex. (b) Čech Complex.

Figure 7: Alpha and Čech complex of the same example set of points in the plane. The alpha complex is a subcomplex of the Čech complex.

The alpha complex is also a subcomplex of the so-called *Delaunay complex*, which is the nerve of the Voronoi sets $\{V_p\}_{p \in P}$. By definition, the alpha complex coincides with the Delaunay complex for large enough values r. One could therefore see the Delaunay complex as the "maximal" alpha complex.

2.2 Alexander Duality

To explore the special case where all the sensors are static in Section 3.1, we will use the standard Alexander Duality Theorem [10],[11]:

Theorem 2. *If K is a locally contractible, compact subset of $\mathbb{R}^d$, then for all $j = 0, ..., d-1$,*

$$\tilde{H}_{d-j-1}(\mathbb{R}^d \setminus K) \cong H^j(K).$$

Example 5. In Subsection 3.1 we will apply Theorem 2 to finite unions of closed balls in $\mathbb{R}^d$. Such a union clearly satisfies the conditions of the theorem, and for $j = d-1$ we get

$$\tilde{H}_0(\mathbb{R}^d \setminus K) \cong H^{d-1}(K).$$

The work of Sara Kališnik [11] provides a parametrized version of Alexander Duality that will be used in the proof of Theorem 6. I will not cover it here, since its statment alone requires more preliminary work that would exceed the scope of this thesis.

2.3 Fibrewise Spaces

This subsection covers fibrewise spaces, following Adams [1] and Crabb [6]. Let I denote the interval $[0, 1]$.

Definition.

- *A **fibrewise space** is a topological space Y together with a continuous map $p : Y \to I$.*
- *Given $t_0 \in I$, the subset $p^{-1}(t_0) \subset Y$ is called the **fibre** over t_0.*
- *Given $[t_0, t_1] \subset I$, we call $p^{-1}([t_0, t_1])$ the **fibre-slice** over $[t_0, t_1]$.*
- *A continuous map $f : Y \to W$ between two fibrewise spaces $p : Y \to I$ and $q : W \to I$ is called **fibrewise**, if the following diagram commutes:*

$$\begin{array}{ccc} Y & \xrightarrow{\quad f \quad} & W \\ & {\scriptstyle p}\searrow \quad \swarrow{\scriptstyle q} & \\ & I & \end{array}$$

, i.e., $q \circ f \equiv p$.

- *Two fibrewise maps $f_0, f_1 : Y \to W$ are **fibrewise homotopic**, if there exists a time-preserving homotopy, i.e. a map $F : Y \times I \to W$ such that $F(-, 0) \equiv f_0$, $F(-, 1) \equiv f_1$, and such that each $F(-, t) : Y \to W$ is fibrewise.*
- *A fibrewise map $f : Y \to W$ is called a **fibrewise homotopy equivalence**, if there exists a fibrewise map $g : W \to Y$ such that $f \circ g$ is fibrewise homotopic to id_W and $g \circ f$ is fibrewise homotopic to id_Y.*
- *Two topological spaces Y and W are called **fibrewise homotopy equivalent**, if there exists a fibrewise homotopy equivalence $f : Y \to W$.*
- *A section for a fibrewise space $p : Y \to I$ is a fibrewise map $s : I \to Y$.*
  Remark: Here we regard I as a fibrewise space with the identity map.

Example 6. An easy way to build a fibrewise space is to take the product $X \times I$, where X is some topological space, and the projection map p onto the second coordinate.

Remark. We can understand a fibrewise space $p : Y \to I$ as a space endowed with a time coordinate. Then, p indicates the time at each point in the "spacetime" Y. This is particularly intuitive in the example above, where $Y = X \times I$ has a "space coordinate" and a time coordinate.
With this understanding, a *fibre* is now just the space at a given point in time, and a *fibre-slice* is the space within a given time interval. Furthermore, a *fibrewise map* is a continuous map from one spacetime into another that satisfies the restriction that each point can only be mapped to a point with the same time coordinate.

2.4 Zigzag Persistence

This subsection intoduces *zigzag modules*, following the work of Carlsson and de Silva [4] in addition to [1]. We will work with vector spaces over a fixed field k.

Definition. *A **zigzag module** V is a diagram*

$$V_1 \overset{q_1}{\longleftrightarrow} V_2 \overset{q_2}{\longleftrightarrow} V_3 \overset{q_3}{\longleftrightarrow} \cdots \overset{q_{n-1}}{\longleftrightarrow} V_n$$

of finitely many vector spaces V_i and linear maps q_i, each going either to the right or to the left.

Example 7. Consider the following example of a zigzag module from [13]:

$$k \xrightarrow{\binom{1}{0}} k^2 \xleftarrow{\binom{1}{1}} k \xleftarrow{(0\ 1)} k^2 \xrightarrow{\left(\begin{smallmatrix}1&0\\0&1\end{smallmatrix}\right)} k^2.$$

Remark. A zigzag module is a special case of the *realization of a quiver*: A diagram

$$\bullet \longleftrightarrow \bullet \longleftrightarrow \bullet \longleftrightarrow \cdots \longleftrightarrow \bullet$$

where each arrow points either to the left or to the right is a special case of a *quiver*, called an A_n-type quiver. Replacing each node with a vector space and each arrow with a linear map is a representation of that quiver, and in our special case exactly the definition of a zigzag module.

Definition. *A zigzag module is associated with a sequence of directions $(d_1, ..., d_{n-1})$ of symbols f and g, where $d_i = f$ means that the map q_i goes forward, and $d_j = g$ means that the map q_j goes backwards. For instance, the zigzag module in Example 7 is associated with the sequence $f\,g\,g\,f$. Each such sequence of directions defines a* ***type*** *τ of zigzag modules, and zigzag modules of that type are called* ***τ-modules****.*

Remark. A special case of a zigzag module is the type $f\,f\,...\,f$, where all arrows point to the right:

$$V_1 \xrightarrow{q_1} V_2 \xrightarrow{q_2} V_3 \xrightarrow{q_3} \cdots \xrightarrow{q_{n-1}} V_n.$$

This is a *persistence module*, an object of interest to topological data analysists.

For the next part, we fix a type τ of zigzag modules.

Definition. *A* ***morphism*** *of τ-modules V and W is a collection f of maps $f_i : V_i \to W_i$ such that all squares in the following diagram commute:*

$$\begin{array}{ccccccccc} V_0 & \longleftrightarrow & V_1 & \longleftrightarrow & \cdots & \longleftrightarrow & V_{n-1} & \longleftrightarrow & V_n \\ \downarrow{\scriptstyle f_0} & & \downarrow{\scriptstyle f_1} & & & & \downarrow{\scriptstyle f_{n-1}} & & \downarrow{\scriptstyle f_n} \\ W_0 & \longleftrightarrow & W_1 & \longleftrightarrow & \cdots & \longleftrightarrow & W_{n-1} & \longleftrightarrow & W_n. \end{array}$$

Furthermore, f is called an ***isomorphism*** *if all f_i are isomorphisms of vector spaces.*

We will later work with zigzag modules consisting of homology groups with field coefficients as vector spaces. Just like in persistent homology, we will be able to get a barcode. Each interval (b, d) with $1 \leq b \leq d \leq n$ in the barcode will represent the following τ-module $\mathbb{I}(b, d)$:

$$0 \longleftrightarrow \cdots \longleftrightarrow 0 \longleftrightarrow K \xleftrightarrow{id} \cdots \xleftrightarrow{id} K \longleftrightarrow 0 \longleftrightarrow \cdots \longleftrightarrow 0.$$

More precicely, such an interval representation $\mathbb{I}(b, d)$ consists of the vector spaces

$$V_i = \begin{cases} K & , b \leq i \leq d \\ 0 & , \text{otherwise} \end{cases}$$

and connecting maps

$$q_i = \begin{cases} \text{id} & , b \leq i \leq d-1 \\ 0 & , \text{otherwise.} \end{cases}$$

The type τ is ommitted from notation since the only relevant aspect of $\mathbb{I}(b, d)$ will be the interval (b, d), the lifespan of a simplex.

Theorem 3 (Gabriel [9])**.** *Every τ-module V is isomorphic to a finite direct sum*

$$\bigoplus_{i=1}^{k} \mathbb{I}(b_i, d_i)$$

of some interval representations of type τ. Furthermore, this decomposition of V is unique up to reordering.

Theorem 3 now allows the definition of a *barcode*:

Definition. *Given a zigzag module $V \cong \oplus_{i=1}^{k} \mathbb{I}(b_i, d_i)$ for some positive integers $1 \leq b_i \leq d_i \leq n$, its* ***barcode*** *is the multiset $\{[b_1, d_1], ..., [b_k, d_k]\}$.*

2.4.1 Levelset Zigzag Persistence

We can build a certain kind of zigzag modules by taking its vector spaces to be homology groups of fibres and fibre-slices, and by taking inclusions of the former into the latter [5]. Seeing a fibrewise space as a space endowed with a time coordinate, this means taking homology groups of that space at different times.

Assume we are given a fibrewise space $p : Y \to I$ that is of *Morse type*, i.e. there are so-called *critical values* $0 < t_1 < ... < t_n < 1$ such that the following conditions hold:

- For each interval
$$J \in \big\{[0, t_1), (t_1, t_2), ..., (t_{n-1}, t_n), (t_n, 1]\big\},$$
the slice $Y_J := p^{-1}(J)$ is homeomorphic to some product of the form $X \times J$ with p corresponding to the projection onto J,
- each homeomorphism $h_J : X \times J \to Y_J$ extends to a continuous function $X \times \bar{J} \to Y_{\bar{J}}$, where $\bar{J}$ denotes the closure of J in $\mathbb{R}$,
- and each slice Y_J has finitely-generated homology.

Given interleaving times
$$0 = s_0 < t_1 < s_1 < ... < t_n < s_n = 1,$$
define subspaces $Y_i := p^{-1}(s_i)$ and $Y_i^{i+1} := p^{-1}([s_i, s_{i+1}])$ for all i in $\{0, ..., n\}$ and i in $\{0, ..., n-1\}$, respectively. Inclusion maps give us the following zigzag diagram:

$$Y_0 \hookrightarrow Y_0^1 \hookleftarrow Y_1 \hookrightarrow ... \hookleftarrow Y_{n-1} \hookrightarrow Y_{n-1}^n \hookleftarrow Y_n.$$

Example 8. Consider the following fibrewise space with the projection map onto the x-axis:

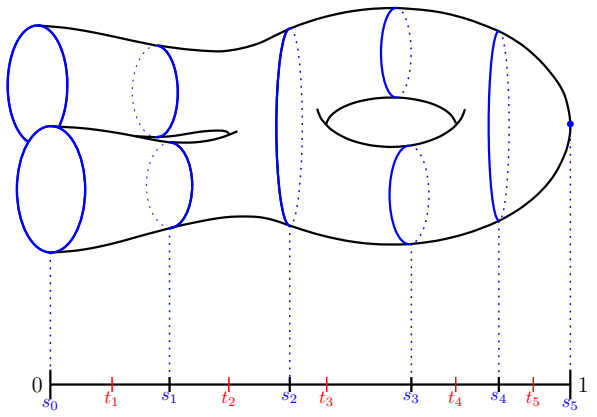

Figure 8: A fibrewise Space separated into five slices.

We choose interleaving times $0 = s_0 < s_1 < s_2 < s_3 < s_4 < s_5 = 1$ to a set of critical times t_i and create fibres separating slices. Inclusions of the fibres into the slices give the following zigzag diagram:

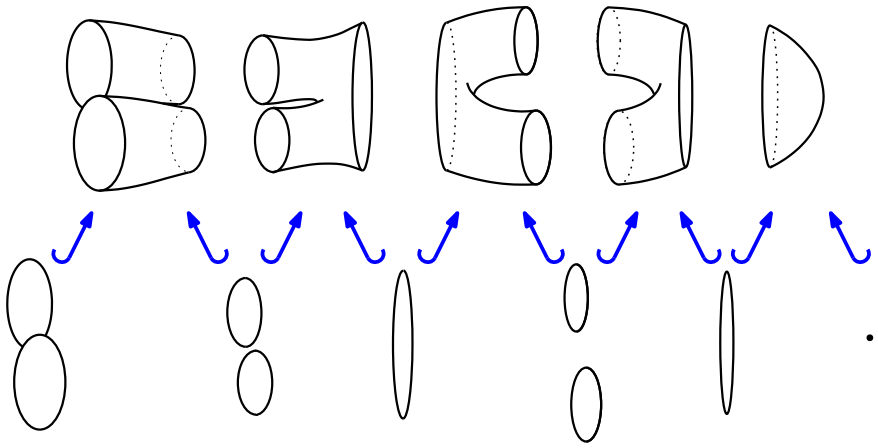

Figure 9: Zigzag diagram from the above fibrewise space.

Inclusion maps induce maps in homology. Taking j-dimensional homology (with coefficients in some fixed field k) of all fibres Y_i and fibre-slices Y_i^{i+1}, we get the following diagram:

$$H_j(Y_0) \hookrightarrow H_j(Y_0^1) \hookleftarrow H_j(Y_1) \hookrightarrow ... \hookleftarrow H_j(Y_{n-1}) \hookrightarrow H_j(Y_{n-1}^n) \hookleftarrow H_j(Y_n). \tag{1}$$

Similarly, taking j-dimensional cohomology, we get

$$H^j(Y_0) \hookleftarrow H^j(Y_0^1) \hookrightarrow H^j(Y_1) \hookleftarrow ... \hookrightarrow H^j(Y_{n-1}) \hookleftarrow H^j(Y_{n-1}^n) \hookrightarrow H^j(Y_n). \tag{2}$$

Note that for cohomology the arrows are reversed, since cohomology is a contravariant functor.

Definition. *Both diagrams are zigzag modules. We call (1)* ***zigzag persistent homology****, denoted by $ZH_j(Y)$, and we call (2)* ***zigzag persistent cohomology****, denoted by $ZH^j(Y)$.*

Example 9. We can now also associate a fibrewise space Y with barcodes, by taking the barcode belonging to its zigzag persistence homology or cohomology. In the example in Figure 8, taking ZH_1, we have one cycle that persist over the interval $[0, t_2]$, one that persists over $[t_3, t_4]$, and one that is present the entire time up until time 1. We therefore get the following barcode:

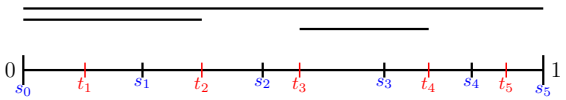

Figure 10: Barcode of the fibrewise space from Figure 8.

Fibrewise maps between fibrewise spaces induce morphisms between zigzag homology and cohomology that satisfy functoriality properties:

Lemma 1. *Let Y and W be two fibrewise spaces, and $f : Y \to W$ a fibrewise map. Then it induces morphisms of zigzag modules*

$$ZH_j(f) : ZH_j(Y) \to ZH_j(W)$$

such that

(1) for fibrewise maps $X \xrightarrow{f} Y \xrightarrow{g} Z$, $ZH_j(g \circ f) = ZH_j(g) \circ ZH_j(f)$,

(2) and $ZH_j(id_X) = id_{ZH_j(X)}$.

Proof. Consider the restrictions $f_i := f|_{Y_i}$ and $f_i^{i+1} := f|_{Y_i^{i+1}}$. By definition of fibrewise maps, they each map into W_i and W_i^{i+1}, respectively. Combining these restrictions with the inclusion-zigzag structure from before, we get the following commutative diagram:

$$\begin{array}{ccccccccccccc}
Y_0 & \hookrightarrow & Y_0^1 & \hookleftarrow & Y_1 & \hookrightarrow & \cdots & \hookleftarrow & Y_{n-1} & \hookrightarrow & Y_{n-1}^n & \hookleftarrow & Y_n \\
\downarrow{\scriptstyle f_0} & & \downarrow{\scriptstyle f_0^1} & & \downarrow{\scriptstyle f_1} & & & & \downarrow{\scriptstyle f_{n-1}} & & \downarrow{\scriptstyle f_{n-1}^n} & & \downarrow{\scriptstyle f_n} \\
W_0 & \hookrightarrow & W_0^1 & \hookleftarrow & W_1 & \hookrightarrow & \cdots & \hookleftarrow & W_{n-1} & \hookrightarrow & W_{n-1}^n & \hookleftarrow & W_n
\end{array}$$

Applying the j-th homology functor, we get another commutative diagram

$$\begin{array}{ccccccccccccc}
H_j(Y_0) & \longrightarrow & H_j(Y_0^1) & \longleftarrow & H_j(Y_1) & \longrightarrow & \cdots & \longleftarrow & H_j(Y_{n-1}) & \longrightarrow & H_j(Y_{n-1}^n) & \longleftarrow & H_j(Y_n) \\
\downarrow{\scriptstyle (f_0)_*} & & \downarrow{\scriptstyle (f_0^1)_*} & & \downarrow{\scriptstyle (f_1)_*} & & & & \downarrow{\scriptstyle (f_{n-1})_*} & & \downarrow{\scriptstyle (f_{n-1}^n)_*} & & \downarrow{\scriptstyle (f_n)_*} \\
H_j(W_0) & \longrightarrow & H_j(W_0^1) & \longleftarrow & H_j(W_1) & \longrightarrow & \cdots & \longleftarrow & H_j(W_{n-1}) & \longrightarrow & H_j(W_{n-1}^n) & \longleftarrow & H_j(W_n),
\end{array}$$

where the collection of the vertical maps makes up a morphism of zigzag modules that we denote by $ZH_j(f)$.

(1) and (2) follow directly from the functoriality of the j-th homology functor. □

The following lemma shows that, similarly to unparametrized homology, zigzag persistent homology and cohomology are invariant under fibrewise homotopy equivalences.

Lemma 2. *If two fibrewise spaces Y and W are fibrewise homotopy equivalent, then they have the same zigzag persistent homology and cohomology up to isomorphism:*

$$ZH_j(Y) \cong ZH_j(W) \quad \textit{and} \quad ZH^j(Y) \cong ZH^j(W).$$

Proof. By definition, there exists a fibrewise homotopy equivalence $f : Y \to W$ with an inverse $g : W \to Y$. f and g are fibrewise maps such that $f \circ g$ and $g \circ f$ are each fibrewise homotopic to the respective identity map.

Like in the previous proof, consider again the restrictions $f_i := f|_{Y_i}$ and $f_i^{i+1} := f|_{Y_i^{i+1}}$. By definition of fibrewise maps, they each map into W_i and W_i^{i+1}, respectively. Therefore, $g|^{Y_i}$ and $g|^{Y_i^{i+1}}$, respectively, work as homotopy inverses, and the f_i and f_i^{i+1} are fibrewise homotopy equivalences.

Combining these restrictions with the inclusion-zigzag structure from before, we get the following commutative diagram:

$$\begin{array}{ccccccccccccc}
Y_0 & \hookrightarrow & Y_0^1 & \hookleftarrow & Y_1 & \hookrightarrow & \cdots & \hookleftarrow & Y_{n-1} & \hookrightarrow & Y_{n-1}^n & \hookleftarrow & Y_n \\
\downarrow{\scriptstyle f_0} & & \downarrow{\scriptstyle f_0^1} & & \downarrow{\scriptstyle f_1} & & & & \downarrow{\scriptstyle f_{n-1}} & & \downarrow{\scriptstyle f_{n-1}^n} & & \downarrow{\scriptstyle f_n} \\
W_0 & \hookrightarrow & W_0^1 & \hookleftarrow & W_1 & \hookrightarrow & \cdots & \hookleftarrow & W_{n-1} & \hookrightarrow & W_{n-1}^n & \hookleftarrow & W_n.
\end{array}$$

Applying homology, we get another commutative diagram

$$\begin{array}{ccccccccccccc}
H_j(Y_0) & \longrightarrow & H_j(Y_0^1) & \longleftarrow & H_j(Y_1) & \longrightarrow & \cdots & \longleftarrow & H_j(Y_{n-1}) & \longrightarrow & H_j(Y_{n-1}^n) & \longleftarrow & H_j(Y_n) \\
\downarrow & & \downarrow & & \downarrow & & & & \downarrow & & \downarrow & & \downarrow \\
H_j(W_0) & \longrightarrow & H_j(W_0^1) & \longleftarrow & H_j(W_1) & \longrightarrow & \cdots & \longleftarrow & H_j(W_{n-1}) & \longrightarrow & H_j(W_{n-1}^n) & \longleftarrow & H_j(W_n),
\end{array}$$

where the vertical maps are induced by homotopy equivalences, and are therefore isomorphisms. This concludes the proof for homology by definition of isomorphic zigzag modules. The proof for cohomology is analogous. □

For the next lemma we will need a version of the *Universal Coefficient Theorem* [10]. Hatcher extends the Universal Coefficient Theorem from chain complexes of free abelian groups to chain complexes of free R-modules for a ring R. Taking R to be a field, one gets the following version of the theorem:

Theorem 4 (Universal Coefficient Theorem for Chain Complexes of Vector Spaces)**.** *Given a chain complex $\mathcal{C}_\bullet$ of vector spaces over a field k, let $H_n(\mathcal{C}_\bullet)$ be the homology groups taken with coefficients in k. For any vector space V over k, we have an isomorphism*

$$H^n(\mathcal{C}_\bullet; V) \xrightarrow{h} \hom_k(H_n(\mathcal{C}_\bullet), V).$$

Remark. This isomorphism comes from a natural short exact sequence

$$0 \to \mathrm{Ext}_k(H_{n-1}(\mathcal{C}_\bullet), V) \to H^n(\mathcal{C}_\bullet; V) \xrightarrow{h} \hom_k(H_n(\mathcal{C}_\bullet), V) \to 0,$$

where the first term is 0 since we are working with a field k and not a general ring. Naturality in our case means that for a chain map $\alpha : \mathcal{C}_\bullet \to \mathcal{D}_\bullet$ between chain complexes of vector spaces, the following diagram commutes:

$$\begin{array}{ccccc}
\mathrm{Ext}_k(H_{n-1}(\mathcal{C}_\bullet), V) & \longrightarrow & H^n(\mathcal{C}_\bullet; V) & \xrightarrow{h} & \hom_k(H_n(\mathcal{C}_\bullet), V) \\
\uparrow{\scriptstyle (\alpha_*)^*} & & \uparrow{\scriptstyle \alpha^*} & & \uparrow{\scriptstyle (\alpha_*)^*} \\
\mathrm{Ext}_k(H_{n-1}(\mathcal{D}_\bullet), V) & \longrightarrow & H^n(\mathcal{D}_\bullet; V) & \xrightarrow{h} & \hom_k(H_n(\mathcal{D}_\bullet), V),
\end{array}$$

where again, the Ext terms are both 0.

Lemma 3. *The barcodes for $ZH_j(Y)$ and $ZH^j(Y)$ are equal as multisets of intervals.*

Proof. According to Theorem 3, there exists a decomposition

$$ZH_j(Y) \cong \bigoplus_{i=1}^{m} \mathbb{I}(b_i, d_i). \tag{3}$$

Dualizing it, i.e. applying the contravariant functor $\hom_k(-, k)$ with $\hom_k$ abbreviated as hom, yields

$$\hom(ZH_j(Y), k) \cong \bigoplus_{i=1}^{m} \hom(\mathbb{I}(b_i, d_i), k) \cong \bigoplus_{i=1}^{m} \mathbb{I}(b_i, d_i), \tag{4}$$

where by applying hom to a zigzag module we mean applying it seperately to every vector space and every linear map of the zigzag module.

The second isomorphism holds since $\hom(0, k) \cong 0$ trivially, and since there exists an isomorphism $\varphi : k \to \hom(k, k)$. We get a commutative diagram

$$\begin{array}{ccccccccccccccc}
0 & \longleftrightarrow & \cdots & \longleftrightarrow & 0 & \longleftrightarrow & k & \longleftrightarrow & \cdots & \longleftrightarrow & k & \longleftrightarrow & 0 & \longleftrightarrow & \cdots & \longleftrightarrow & 0 \\
\cong\downarrow{\scriptstyle 0} & & & & \cong\downarrow{\scriptstyle 0} & & \cong\downarrow{\scriptstyle \varphi} & & & & \cong\downarrow{\scriptstyle \varphi} & & \cong\downarrow{\scriptstyle 0} & & & & \cong\downarrow{\scriptstyle 0} \\
\hom(0,k) & \leftrightarrow & \cdots & \leftrightarrow & \hom(0,k) & \leftrightarrow & \hom(k,k) & \leftrightarrow & \cdots & \leftrightarrow & \hom(k,k) & \leftrightarrow & \hom(0,k) & \leftrightarrow & \cdots & \leftrightarrow & \hom(0,k)
\end{array}$$

with all vertical maps being isomorphisms. Note that applying hom to a zigzag module changes all the directions of the arrows. So even though it is ommitted in notation, the $\mathbb{I}(b_i, d_i)$ in (3) are not the same zigzag modules as in (4).

The lefthand side of (4) now looks like this:

$$\hom(H_j(Y_0), k) \leftarrow \hom(H_j(Y_0^1), k) \rightarrow \hom(H_j(Y_1), k) \leftarrow \cdots \rightarrow \hom(H_j(Y_n), k).$$

Applying the Universal Coefficiant Theorem 4 to chain complexes of the spaces Y_i and Y_i^{i+1} yields isomorphisms

$$H^j(Y_i^{(i+1)}; k) \xrightarrow{h} \hom(H_j(Y_i^{(i+1)}), k).$$

Naturality in the Universal Coefficiant Theorem gives a commutative diagram

$$\begin{array}{ccccccccc}
H^j(Y_0; k) & \longleftarrow & H^j(Y_0^1; k) & \longrightarrow & H^j(Y_1; k) & \longleftarrow & \cdots & \longrightarrow & H^j(Y_n; k) \\
\cong\downarrow h & & \cong\downarrow h & & \cong\downarrow h & & & & \cong\downarrow h \\
\hom(H_j(Y_0), k) & \longleftarrow & \hom(H_j(Y_0^1), k) & \longrightarrow & \hom(H_j(Y_1), k) & \longleftarrow & \cdots & \longrightarrow & \hom(H_j(Y_n), k),
\end{array}$$

which concludes the proof together with (4). □

3 Sensor Networks and Coverage of Static Sensor Networks

Let us now generalize the situation from the introduction. This section follows [1].

Consider a space $\mathcal{D}$ that is homotopy equivalent to a d-dimensional disc. We formally define a *sensor* as a path $v : I \to \mathcal{D}$ that represents the route a sensor takes in the domain. Finally, let $S = \{v_1, ..., v_n\}$ be a finite set of sensors and assume $v_i(t) \neq v_j(t) \ \ \forall 1 \leq i \neq j \leq n \ \forall t \in I$.

In addition to the positions of the sensors as time changes, we need to define the observed area by a sensor. For reasons of simplicity, assume that each sensor observes exactly the area in the ball $B_{v(t)}$ with radius 1 around itself.

An example for $\mathcal{D} = \mathbb{D}^2$ and just three sensors may look like Figure 11.

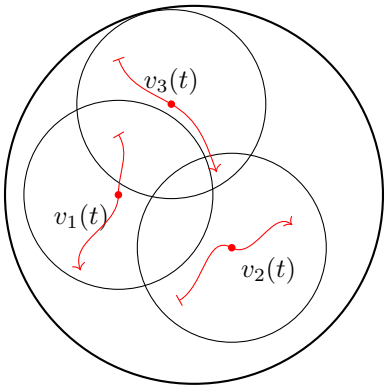

Figure 11: Example of 3 sensors at a fixed time t. The nodes $\bullet$ represent the current positions, each with a ball $B_{v(t)}$ around them. The arrows $\longmapsto$ represent the path a sensor follows in the time interval I.

The nodes with balls around them invite us to construct a Čech complex: a subset $\{v_{i_0}, ..., v_{i_k}\}$ of sensors determines a k-simplex at time t exactly if they all observe some common non-empty area, i.e. if

$$B_{v_{i_0}(t)} \cap B_{v_{i_1}(t)} \cap \cdots \cap B_{v_{i_k}(t)} \neq \varnothing.$$

We denote this Čech complex at time t by $C(t)$.

In our example, we get a 2-simplex and all of its faces (see Figure 12(a)). This gives information about the area between the sensors, but not about the area between the "outmost" sensors and the boundary of $\mathcal{D}$. Therefore, we introduce stationary fence sensors on the boundary such that $\partial\mathcal{D}$ is included in their observation balls (see Figure 12(b)). The resulting Čech complex (Figure 12(c)) now contains information about the entire domain.

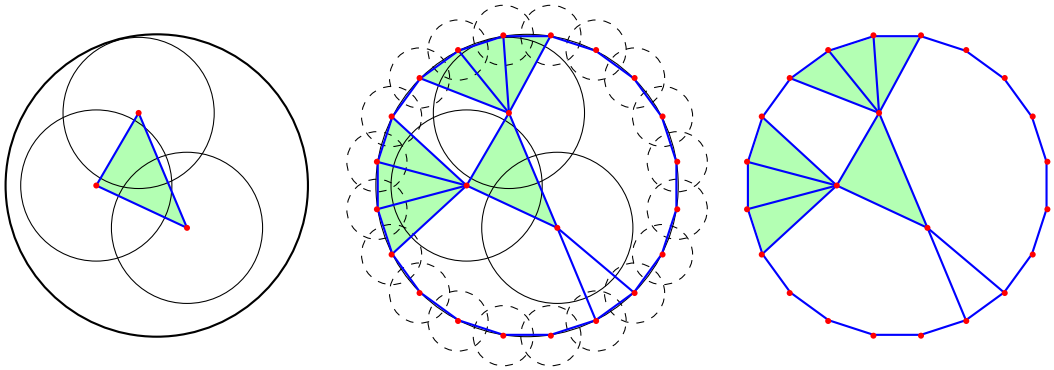

(a) (b) (c)

Figure 12: Čech complex of example from Figure 11 and Čech complex including boundary sensors.

As explained in the introduction, we are interested in the area that is covered by the sensors, or not covered, respectively. Thus, we define the following:

Definition. *Let*

$$X(t) := \bigcup_{v \in S} B_{v(t)}$$

be the ***covered area at time*** t*, and let*

$$X(t)^C := \mathcal{D} \setminus X(t)$$

be the ***uncovered area at time*** t*.*

Naturally, the collection $\{B_{v(t)}\}_{v \in S}$ is a covering of $X(t)$, and since the Čech complex $C(t)$ is defined to be the nerve of that same collection, we can apply the Nerve Theorem (Theorem 1) and get the following important property: At any given time t, the Čech complex $C(t)$ is homotopy equivalent to the covered region $X(t)$.

In order to observe what happens as time passes, we add a time coordinate:

Definition. *Let*

$$X := \bigcup_{t \in I} X(t) \times t \ \subset \mathcal{D} \times I$$

be the ***covered area in spacetime****, and let*

$$X^C := \mathcal{D} \times I \setminus X$$

be the ***uncovered area in spacetime****.*

Remark. Note that both X and X^C are fibrewise spaces when endowed with the projection map $p : \mathcal{D} \times I \to I$ restricted to X and X^C, respectively.

Before formalizing the evasion problem from the introduction, we take a look at the special case where all the sensors are static.

3.1 Special case: static sensors

In the case where all sensors are static, i.e. $v(t) = v \in \mathcal{D}$ is constant for all $v \in S$, the evasion problem becomes much simpler. The question is now whether $\{B_v\}_{v \in S}$ covers $\mathcal{D}$.

In the 2-dimensional case, the situation may look like this:

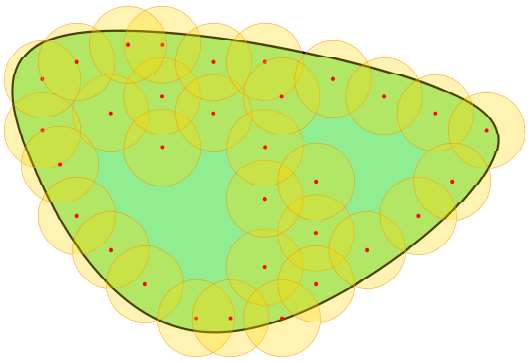

Figure 13: A static sensor network.

Let $K = X(0) = \bigcup_{v \in S} B_v$ be the (constant) covered area by the sensors, and let $C := C(0)$ be the (constant) Čech complex of the covering by the sensor balls B_v. The domain is fully covered exactly

when the complement $K^C := \mathcal{D} \setminus K$ of the covered area is empty, or in other words, has zero connected components. This is the case if and only if

$$0 = \dim H_0(K^C) = \dim H_0(\mathbb{R}^d \setminus K) - 1 = \dim \tilde{H}_0(\mathbb{R}^d \setminus K).$$

Here, as in the rest of this thesis, we take homology groups with coefficients in a field. Applying Alexander Duality yields:

$$\tilde{H}_0(\mathbb{R}^d \setminus K) \cong H^{d-1}(K) \cong H^{d-1}(C)$$

Thus, the sensors provide a cover for $\mathcal{D}$ if and only if $\dim H^{d-1}(C) = 0$.

Example 10. In the static sensor network in 13, we have two connected components in K^C, and three in $\mathbb{R}^2 \setminus K$. In particular, $\dim H_0(K^C) \neq 0$, and clearly the sensors do not provide a covering of $\mathcal{D}$.

In the next section we will explore whether the time-varying Čech complex $C(t)$ is also sufficient in the non-static case to answer the question of whether an "evasion path" exists.

4 The Evasion Problem

In this section we are coming back to our question from the introduction: Is it possible for an intruder to evade the sensors in a mobile sensor network?

Let us begin by formally defining the matter of "evading the sensors":

Definition. *Given a sensor network $(\mathcal{D}, S)$ as introduced in the previous section, define an* ***evasion path*** *to be a section of $p : X^C \to I$.*

The definition of an evasion path s as a section of a fibrewise space translates a "sensor-avoiding" path $I \to \mathcal{D}$ into a path $s : I \to X^C$ in spacetime that respects the time-coordinate. A regular path in spacetime $\mathcal{D} \times I$ only needs to be continuous, but can go back and forth in time as much as it wants. A section, and thus an evasion path, intersects each fibre at exactly the point in time that corresponds to that fibre.

Example 11. Consider the following examples of sensor networks, where the domain is a two-dimensional disc, the observed area is depicted in orange, and the time is depicted horizontally:

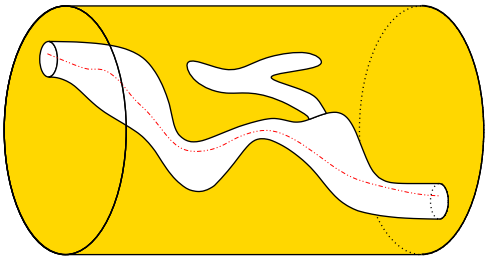

Figure 14: In this sensor network, an evasion path exists.

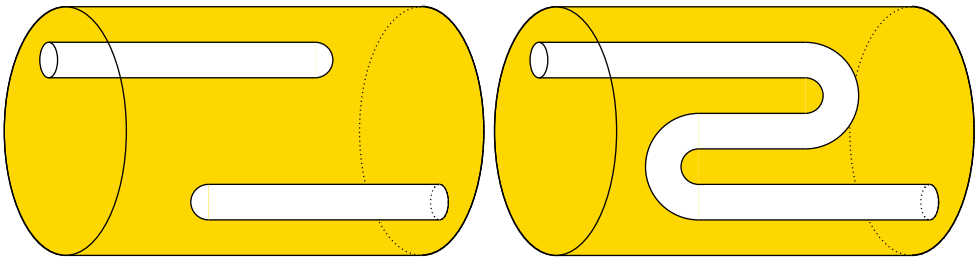

(a) (b)

Figure 15: In both (a) and (b) no evasion path exists.

In the example in Figure 14, a possible evasion path is marked. However, in Figure 15(a), there exists no path in spacetime that connects the fibre at 0 and the fibre at 1, so an evasion path cannot possibly exist. In 15(b), such paths do exist, but they all go back and forth in time, and therefore cannot be evasion paths. Formally, they are maps from I into the uncovered area in spacetime, but they are not fibrewise.

The question is now whether or not such an evasion path exists for any given network. As in [1], we approach this question by looking at the time-varying Čech complex $C(t)$:

Main question: Given the time-varying Čech complex $C(t)$ for all $t \in I$ of a sensor network $(\mathcal{D}, S)$, can we determine whether or not an evasion path exists?

Assumptions:

1. The Čech complex $C(t)$ changes only at finitely many times $0 < t_1 < \cdots < t_n < 1$.

2. At each time t_i, there are either only simplices added, or only simplices removed, but not both.

Note that since the sensor balls are closed, "added at t_i" means the simplex is present at time t_i but not right before, and "removed at t_i" means the simplex is present at time t_i but not right after.

4.1 Stacked Čech Complexes

In order to investigate how the Čech complex changes over time, we choose interleaving times

$$0 = s_0 < t_1 < s_1 < \cdots < t_n < s_n = 1,$$

and we construct the so-called *stacked Čech complex*.

Definition. *The **stacked Čech complex** is a fibrewise space $p : SC \to I$, where SC is the disjoint union*

$$\bigsqcup_{i=0}^{n} C(s_i) \times [t_i, t_{i+1}] \quad (t_0 := 0, t_{n+1} := 1)$$

under identification of

- *$C(s_{i-1}) \times \{t_i\}$ as a subset of $C(s_i) \times \{t_i\}$ if simplices are added at t_i, and*
- *$C(s_i) \times \{t_i\}$ as a subset of $C(s_{i-1}) \times \{t_i\}$ if simplices are removed at t_i,*

and p is the projection map onto the second coordinate.

Example 12. Consider a simple example with 3 mobile sensors in the plane. At each time $t \in I$, the three balls around the sensor determine a Čech complex $C(t)$. Assume that the Čech complex changes only three times at $0 < t_1 < t_2 < t_3 < 1$. At interleaving times $0 = s_0 < t_1 < s_1 < t_2 < s_2 < t_3 < s_3 = 1$ the situation may look like this:

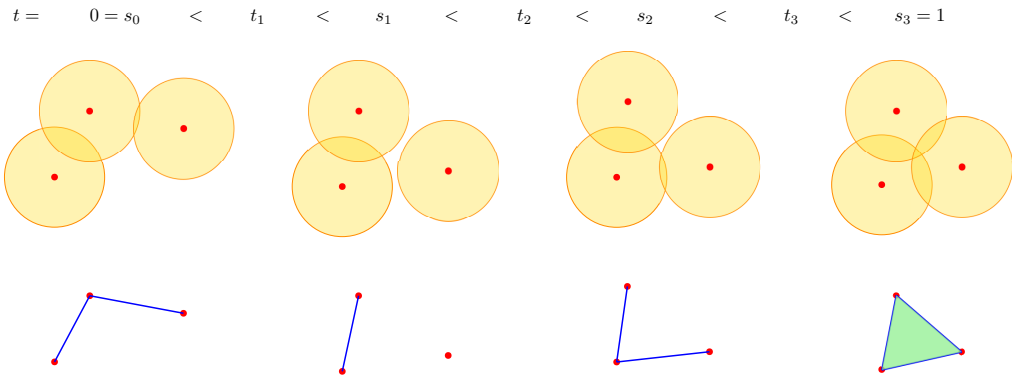

Figure 16: A simple sensor network and its time-varying Čech complex at 4 interleaving times.

Each of the four Čech complexes $C(t_i)$ is constant in the intervals $[0 = s_0, t_1]$, (t_1, t_2), $[t_2, t_3)$, $[t_3, s_3 = 1]$, respectively. The openness or closedness of an interval is determined by whether simplices are added or removed at time t_i. By our assumption, the two cannot happen at the same time. For example, at time t_1 a 1-simplex is removed from the Čech complex. Since the sensor balls are closed, the 1-simplex is still present at time t_1, but not right after.

To construct the stacked Čech complex, we take the disjoint union

$$C(s_0) \times [0, t_1] \;\sqcup\; C(s_1) \times [t_1, t_2] \;\sqcup\; C(s_2) \times [t_2, t_3] \;\sqcup\; C(s_3) \times [t_3, 1]$$

as in Figure 17,

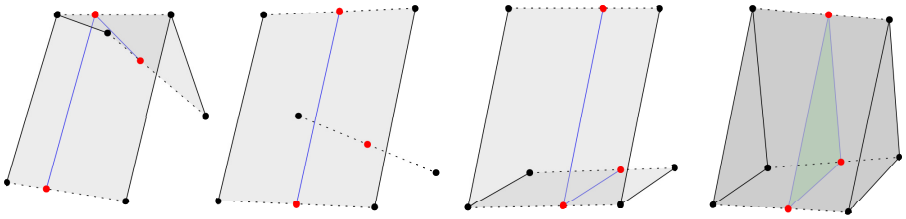

Figure 17: Building the stacked Čech complex via a disjoint union.

and identify the fibres at times t_i via inclusions, as in Figure 18.

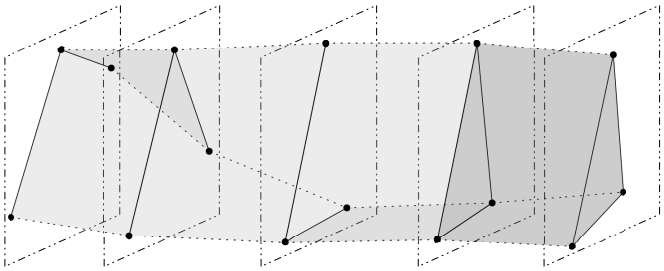

Figure 18: Stacked Čech complex.

The following theorem from the work of V. de Silva and R. Ghrist [7], and reformulated by Henry Adams [1], is the first main theorem in this thesis. It uses the stacked Čech complex and works with the fence sensors to give a necessary condition for the existence of an evasion path. Let $F \times [0,1] \subset SC$ be the subset of the stacked Čech complex that consists only of the immobile fence sensors.

Theorem 5. *If there exists some* $[\alpha] \in H_d(SC, F \times [0,1])$ *with* $0 \neq [\partial\alpha] \in H_{d-1}(F \times [0,1])$*, then there does not exist an evasion path in the sensor network.*

In the following I will try to give some intuition: If there exists some $[\alpha] \in H_d(SC, F \times [0,1])$ with $0 \neq [\partial\alpha] \in H_{d-1}(F \times [0,1])$, then it has a cycle representative α in SC. By definition of a relative cycle, $\partial\alpha$ lies fully in $F \times [0,1]$. But since $[\partial\alpha] \neq 0$ by assumption, it has to "wrap" around $F \times [0,1]$ at least once. Figure 19 shows what the subcomplex $F \times [0,1]$ may look like and presents an example and a counterexample to the condition $[\partial\alpha] \neq 0$.

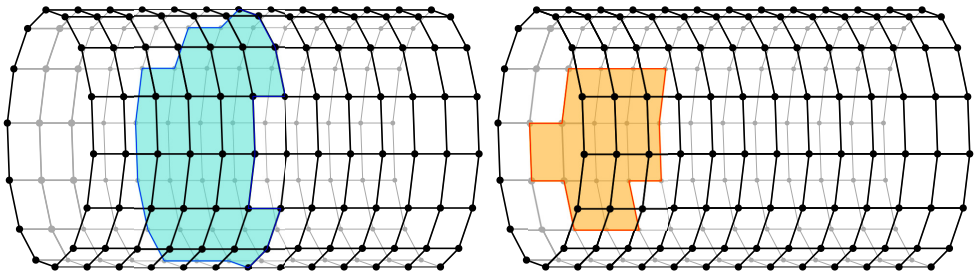

(a) (b)

Figure 19: Illustration of $F \times [0,1]$ and possible d-dimensional cycles in $S_d(SC, F \times [0,1])$. The blue cycle in (a) representing an element in $H_d(SC, F \times [0,1])$ satisfies the conditions from Theorem 5, as its boundary "wraps around" F. The orange cycle in (b), however, does not satisfy the conditions from Theorem 5, as its boundary is trivial in $H_{d-1}(F \times [0,1])$.

Whenever the conditions of Theorem 5 are satisfied, as in Figure 19(a), the cycle can be imagined to be a sheet that is spanning across the domain in spacetime like a membrane, making it impossible for

a potential evasion path to get past. In Figure 19(b), where the condition is not satisfied, on the other hand, an evasion path can easily get past the sheet.

Looking back to the two counterexamples in Figure 15 from Example 11, this theorem would explain why there cannot be an evasion path in (a). However, it does not cover why there is no evasion path in (b). Indeed, Theorem 5 gives a necessary but not sufficient condition for the existence of an evasion path. This insufficiency will be discussed further in Section 4.3.

4.2 Applying Zigzag Homology

In Section 2 we have seen how a zigzag module can be created from a fibrewise space. Let us now apply this procedure to the stacked Čech complex.

Example (Example 12, continued). For the stacked Čech complex from Example 12 we get the following zigzag diagram:

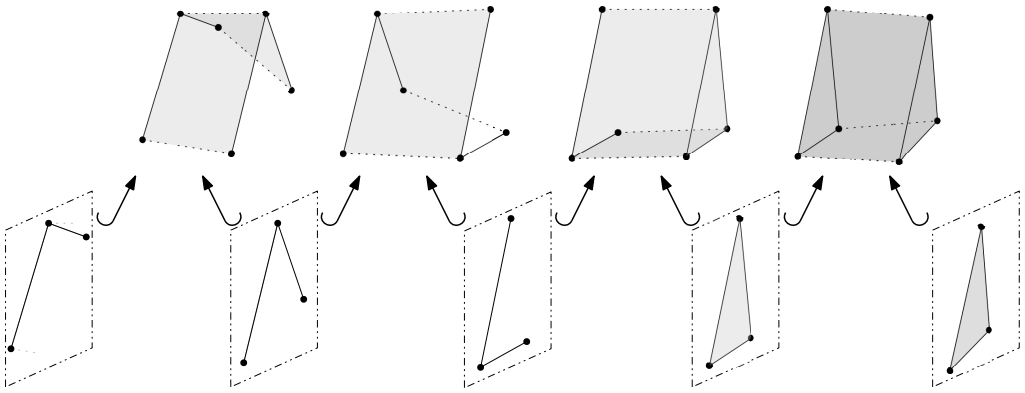

Figure 20: Zigzag diagram from a stacked Čech complex.

The following lemma shows that the stacked Čech complex has the same zigzag homology as the covered area X in spacetime.

Lemma 4. $ZH_j(X) \cong ZH_j(SC)$.

Proof. The fibres are by definition of the stacked Čech complex exactly the Čech complexes at times s_i:

$$SC_i = p^{-1}(s_i) = C(s_i).$$

Similarly, the slices are

$$SC_i^{i+1} = p^{-1}([t_i, t_{i+1}]) = C(s_i) \times [t_i, t_{i+1}].$$

By the Nerve Theorem (Theorem 1), $SC_i = C(s_i)$ is homotopy equivalent to $X(s_i) = X_i$, and thus we also get a homotopy equivalence

$$SC_i^{i+1} = C(s_i) \times [t_i, t_{i+1}] \simeq X(s_i) \times [t_i, t_{i+1}] = X_i^{i+1}.$$

We have a commutative diagram

$$\begin{array}{ccccccccccc}
SC_0 & \hookrightarrow & SC_0^1 & \hookleftarrow & SC_1 & \hookrightarrow & \cdots & \hookleftarrow & SC_{n-1} & \hookrightarrow & SC_{n-1}^n & \hookleftarrow & SC_n \\
\downarrow & & \downarrow & & \downarrow & & & & \downarrow & & \downarrow & & \downarrow \\
X_0 & \hookrightarrow & X_0^1 & \hookleftarrow & X_1 & \hookrightarrow & \cdots & \hookleftarrow & X_{n-1} & \hookrightarrow & X_{n-1}^n & \hookleftarrow & X_n,
\end{array}$$

where each vertical map is a homotopy equivalence. Taking homology, we get a commutative diagram

$$\begin{array}{ccccccccccccc}
H_j(SC_0) & \hookrightarrow & H_j(SC_0^1) & \hookleftarrow & H_j(SC_1) & \hookrightarrow & \cdots & \hookleftarrow & H_j(SC_{n-1}) & \hookrightarrow & H_j(SC_{n-1}^n) & \hookleftarrow & H_j(SC_n) \\
\cong\downarrow & & \cong\downarrow & & \cong\downarrow & & & & \cong\downarrow & & \cong\downarrow & & \cong\downarrow \\
H_j(X_0) & \hookrightarrow & H_j(X_0^1) & \hookleftarrow & H_j(X_1) & \hookrightarrow & \cdots & \hookleftarrow & H_j(X_{n-1}) & \hookrightarrow & H_j(X_{n-1}^n) & \hookleftarrow & H_j(X_n),
\end{array}$$

where all vertical maps are isomorphisms, which concludes the proof. □

Lemma 4 allows us to prove the following theorem. It gives another sufficient condition for the existence of an evasion path, this time using zigzag homology.

Theorem 6. *Consider a sensor network $(\mathcal{D}, S)$ with $\mathcal{D}$ a d-dimensional domain. If there exists an evasion path, then there is a full-length interval $[1, 2n+1]$ in the zigzag barcode for $ZH_{d-1}(SC)$.*

Proof. An evasion path is a a map $s : I \to X^C$ such that the diagram

$$\begin{array}{ccccc}
I & \xrightarrow{s} & X^C & \xrightarrow{p} & I \\
& \searrow & & \nearrow & \\
& & \mathrm{id} & &
\end{array}$$

commutes. By applying 0-dimensional zigzag homology ZH_0, and using functoriality from Lemma 1, we get the commutative diagram

$$\begin{array}{ccccc}
ZH_0(I) & \xrightarrow{ZH_0(s)} & ZH_0(X^C) & \xrightarrow{ZH_0(p)} & ZH_0(I). \\
& \searrow & & \nearrow & \\
& & \mathrm{id} & &
\end{array}$$

So clearly, the identity map on $ZH_0(I)$ factors through $ZH_0(I)$. By definition, $ZH_0(I)$ is the zigzag module

$$\begin{array}{ccccccccccccc}
H_0(I_0) & \hookrightarrow & H_0(I_0^1) & \hookleftarrow & H_0(I_1) & \hookrightarrow & \cdots & \hookleftarrow & H_0(I_{n-1}) & \hookrightarrow & H_0(I_{n-1}^n) & \hookleftarrow & H_0(I_n) \\
\| & & \| & & \| & & & & \| & & \| & & \| \\
H_0([s_0]) & & H_0([s_0, s_1]) & & H_0([s_1]) & & \cdots & & H_0([s_{n-1}]) & & H_0([s_{n-1}, s_n]) & & H_0([s_n]) \\
\cong\downarrow & & \cong\downarrow & & \cong\downarrow & & & & \cong\downarrow & & \cong\downarrow & & \cong\downarrow \\
K & \xhookrightarrow{id} & K & \xhookleftarrow{id} & K & \xhookrightarrow{id} & \cdots & \xhookleftarrow{id} & K & \xhookrightarrow{id} & K & \xhookleftarrow{id} & K,
\end{array}$$

which is isomorphic to exactly $\mathbb{I}(1, 2n+1)$. By the Splitting Lemma (see Section 2.2 in [10]), the short exact sequence

$$0 \longrightarrow ZH_0(I) \xrightarrow{ZH_0(s)} ZH_0(X^C) \xrightarrow{q} \operatorname{Coker} ZH_0(s) \longrightarrow 0$$

is split. Note that the quotient map q and $\operatorname{Coker} ZH_0(s)$ were chosen to complete the sequence to a short exact sequence, but they could be replaced by any vector space and map that satisfy these conditions. Since the sequence is split, there exists an isomorphism

$$ZH_0(X^C) \cong ZH_0(I) \oplus \operatorname{Coker} ZH_0(s) \cong \mathbb{I}(1, 2n+1) \oplus \operatorname{Coker} ZH_0(s).$$

By the uniqueness of the barcode decomposition, there is thus a full-length interval $[1, 2n+1]$ in the barcode for $ZH_0(X^C)$. A parametrized version of Alexander Duality by [11] can be used to show that there is a full-length interval in the zigzag barcode of $ZH^{d-1}(X)$. By Lemma 3 the same must hold for $ZH_{d-1}(X)$, and since $ZH_{d-1}(X) \cong ZH_{d-1}(SC)$ by Lemma 4, we obtain a full-length interval in the zigzag barcode for $ZH_{d-1}(SC)$ as desired. □

4.3 Insufficiency

We have seen Theorems 5 and 6 giving sufficient conditions for the existence of an evasion path.

It turns out that neither of them are sharp enough to give a necessary and sufficient condition. In fact, given a sensor network, neither its time-varying Čech compex nor its fibrewise homotopy type are sufficient to fully determine whether or not an evasion path exists.

To see this, consider the following example (Figure 21(a)) and one of the previous counterexamples (Figure 21(b)).

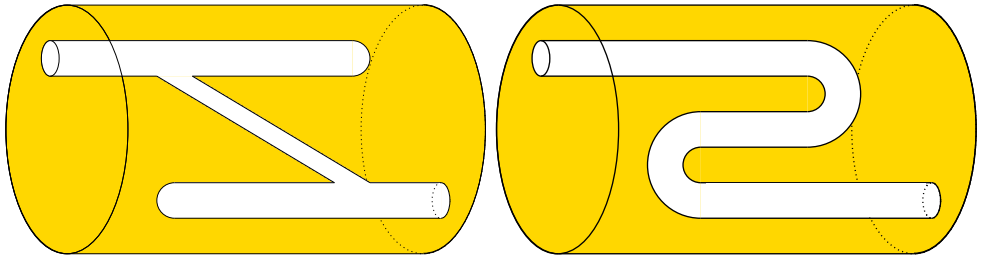

(a) (b)

Figure 21: There exists an evasion path in (a), but not in (b). However, the two have the same fibrewise homotopy type, and their underlying sensor networks may also have the same time-varying Čech complexes.

Figure 22 shows two sequences of Čech complexes, giving an idea of what the (identical) Čech complexes of (a) and (b) from Figure 21 may look like at interleaving times.

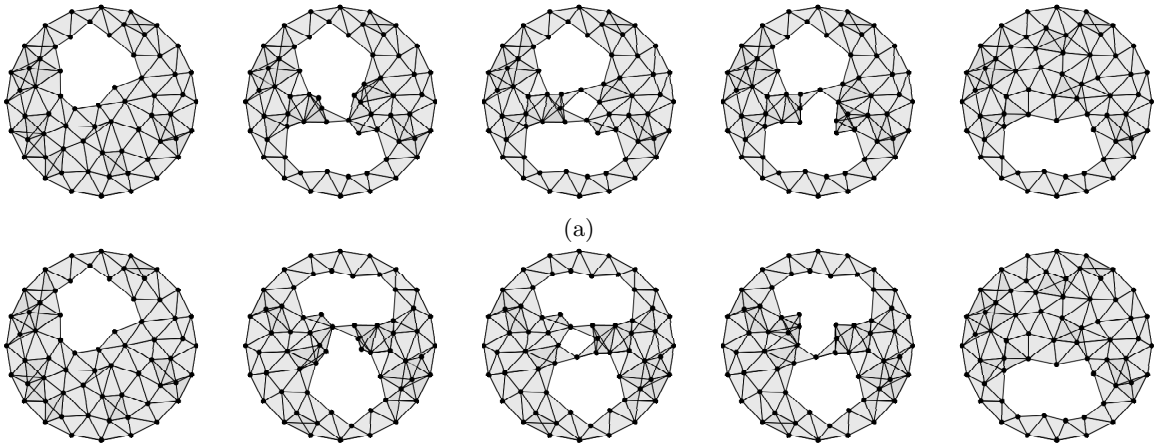

(a)

(b)

Figure 22: Identical sequences of Čech complexes, where an evasion path can exist in (a), but not in (b).

Since an evasion path does exist in (a), by Theorem 5, there cannot exist $[\alpha] \in H_d(SC, F \times [0,1])$ such that with $0 \neq [\partial\alpha] \in H_{d-1}(F \times [0,1])$. And by Theorem 6, there has to be a full-length interval in the zigzag barcode for $ZH_{d-1}(SC)$. But since the mobile sensor networks (a) and (b) have identical time-varying Čech complexes, (b) must also satisfy these two conditions. Meaning that neither of the two theorems can possibly determine that there does not exist an evasion path in (b).

This means that not only are Theorems 5 and 6 not sharp enough to solve the evasion problem, but there cannot exist a sharp theorem that relies only on the fibrewise homotopy type and the time-varying Čech complex. Therefore, the answer to our main question from the beginning of this section is no: Given only

the time-varying Čech complex of a sensor network, it is in general not possible to determine whether or not an evasion path exists.

4.4 Sharp criterion in two dimensions

In the two-dimensional case, Henry Adams resolves the evasion problem by adding more sensor capabilities. In addition to collecting the connectivity data of the sensor networks, the sensors may now also gather the cyclic ordering of neighbours around each sensor. In other words, for each sensor we now know the order in which its incident edges in the connectivity graph appear when going around in clockwise direction. In addition to connectivity and cyclic orderings, the sensors may now also measure the local distances to their neighbours such that we can work with alpha complexes instead of Čech complexes. The crucial advantage here is that the 1-skeleton of the alpha complex is usually planar, whereas the 1-skeleton of the Čech complex does not necessarily need to be. By saying "usually" we mean that there are exceptions. In particular, the special case where the sensor nodes form a regular polygon, for which the 1-skeleton of the alpha complex is not embedded in the plane. We shall neglect these exceptions.

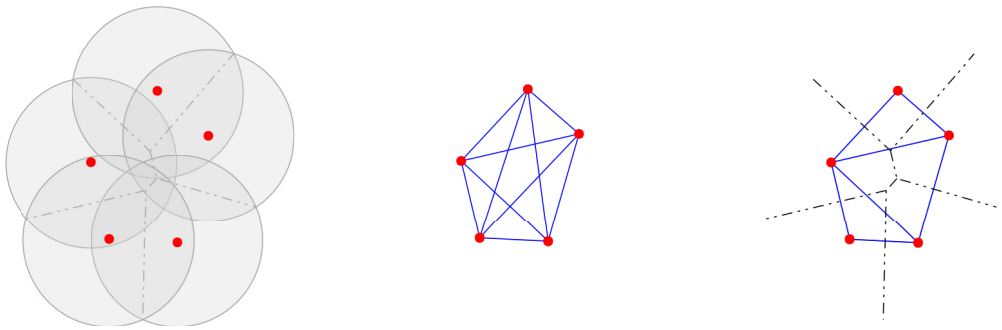

(a) (b) (c)

Figure 23: For the sensor network in (a), we have the 1-skeleton of the Čech complex (b), and of the alpha complex (c). Graph (b) is the complete graph with 5 vertices and non-planar, whereas graph (c) is clearly planar.

The planarity for sensor nodes in general position is easy to see from the construction. In particular, the 1-skeleton of the alpha complex is a subcomplex of the 1-skeleton of the Delaunay complex. If no k sensor nodes for some $k > 3$ form a regular k-gon, then the 1-skeleton of the Delaunay complex corresponds to the dual dual graph of the Voronoi diagram, and is thus, being the dual of a planar graph, planar. For the Čech complex, on the other hand, one can always choose a big enough radius, relative to the pairwise distances of sensors, to get a 1-skeleton that corresponds to a complete graph. For 5 and more sensors, this graph will no longer be planar.

Theorem 7. *Let $(\mathcal{D}, S)$ be a planar sensor network such that the covered region $X(t)$ is connected at each time $t \in I$. Given the time-varying alpha complex and the time-varying cyclic orderings of the neighours of each sensor, we can determine whether or not an evasion path exists.*

Setup for the proof: Let $A^1(t)$ be the 1-skeleton of the time-varying alpha complex of the sensor nodes. It constitutes a simple, planar graph, with the 0-simplices that represent the sensor nodes as vertices, and with the 1-simplices as edges.

The cyclic orderings of incident edges to each vertex give rise to a certain rotation structure of $A^1(t)$. If we view each edge as a pair of two directed edges, one in each direction, we get a partition of $A^1(t)$ into boundary cycles in the following way: a boundary cycle is a cyclic sequence of directed edges $(e_1, e_2, ..., e_k) = ([v_1, v_2], [v_2, v_3], ..., [v_k, v_1])$, where in the (clockwise) cyclic ordering, e_{i+1} is the successor of e_i for all $i = 1, ..., k$ and $k + 1 = 1$.

Example 13. The following figure shows two exemplary boundary cycles of the alpha complex from Figure 23.

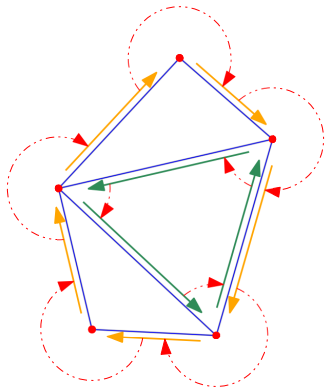

Figure 24: Rotation structure and two exemplary boundary cycles.

With $A^1(t)$ being embedded in the plane, we have a bijective correspondence between these boundary cycles and the connected components of $\mathbb{R}^2 \setminus A^1(t)$. The strategy of the proof is now to determine after each change in the alpha complex for each cycle whether, based on the change and the situation before, it is possible for an intruder to be inside that cycle. If there still exists a cycle for the intruder to be in at the very end, an evasion path exists, and otherwise it does not.

As an example, using such a strategy one could indeed distinguish between the complexes in Figure 22 (of course, the actual proof would only work if the Čech complexes were planar at every point in time).

Similarly to the beginning of this section and in addition to the assumption that no regular polygons occur, we now want to make further assumption about the occurence of changes in the alpha complex.

Assumptions:

1. At all times t, and for all $k > 3$, no k sensor nodes form a regular polygon.
2. The alpha complex changes only at finitely many times $0 < t_1 < ... < t_n < 1$.
3. At each time t_i only one of the following changes happens:
   (I) a single edge is added or removed,
   (II) a single 2-simplex is added or removed,
   (III) a free pair consisting of a 2-simplex and a face edge with no other cofaces is added or removed,
   (IV) or a Delaunay edge flip occurs.

We can now proceed to the proof of the theorem.

Proof. At time 0, label each cycle with either *true* or *false*, stating the possibility of an intruder staying in that cycle, i.e., assign the label *false* to all cycles that are filled in by a 2-simplex, and assign the label *true* to all other cycles. Whenever a change to the alpha complex happens at time t_i, we adapt the labels in the following way:

(I) If a single edge is added, the situation will look something like in Figure 25:

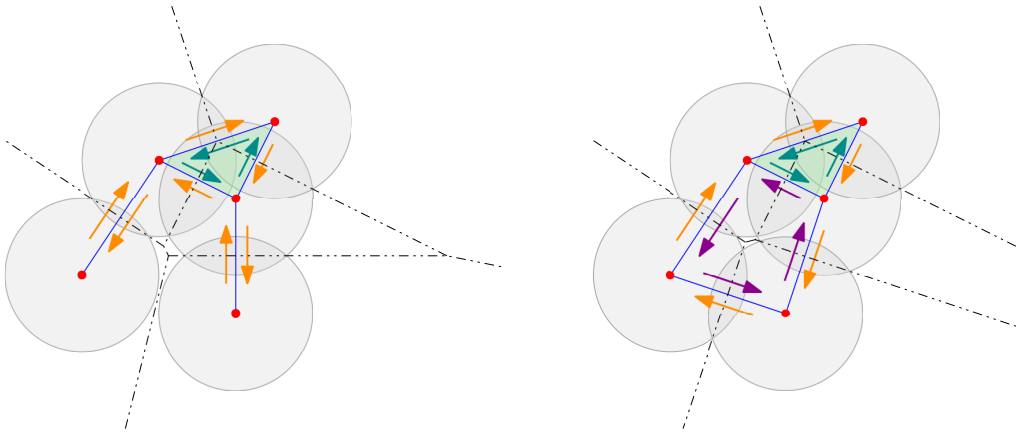

(a) (b)

Figure 25

A single boundary cycle splits into two, since $X(t)$ is connected. If an intruder was inside the cycle before, it can now be in both of the new cycles as well. Thus, the two emerging cycles adapt the label of their parent cycle. Similarly, if a single edge is removed, two cycles merge into one, which we label *true* if and only if at least one of the two parent cycles were labeled *true*.

(II) If a single 2-simplex is added or removed, the situation will look something like in Figure 26:

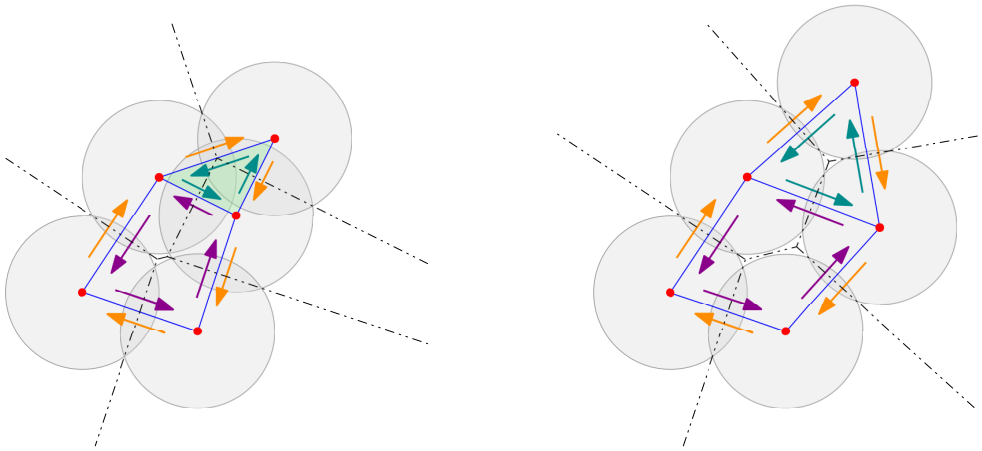

(a) (b)

Figure 26

If it is added, the corresponding cycle of length gets filled in, and we assign the label *false*. If the 2-simplex is removed, then the label on the corresponding boundary cycle shall remain *false*.

(III) If a free pair consisting of a 2-simplex and a face edge is added, then the situation will look something like in Figure 27

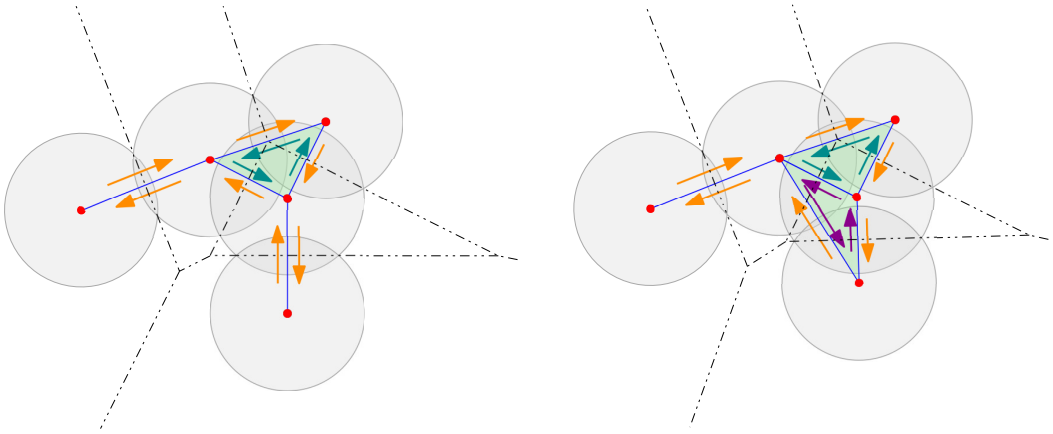

(a) (b)

Figure 27

One boundary cycle splits into two. Naturally, we set the label of the cycle corresponding to the added 2-simplex to *false*, and the other cycle shall keep the label of its parent cycle. Similarly, if the pair is removed, two boundary cycles transform into one, which inherits the label of the parent cycle that did not correspond to the removed 2-simplex.

(IV) If a Delaunay edge flip occurs, the situation will look something like in Figure 28:

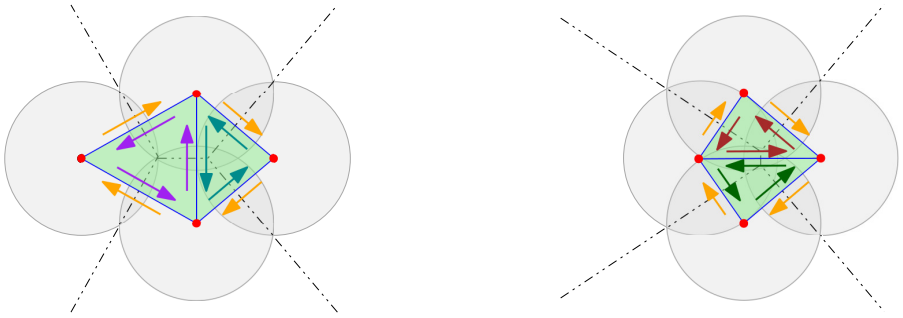

(a) (b)

Figure 28

Two boundary cycles transform into two other boundary cycles. But since they are all filled in, the new cycles will also be labeled *false*.

Through this procedure, the labels will at each time correctly state whether an intruder can or cannot be present in the cycle. If, at time 1, at least one cycle is labeled *true*, then there exists an evasion path. Otherwise, no evasion path can exist. □

References

[1] Henry Adams and Gunnar Carlsson. Evasion paths in mobile sensor networks. *The International Journal of Robotics Research*, 34(1):90–104, 2015.

[2] Karol Borsuk. On the imbedding of systems of compacta in simplicial complexes. *Fundamenta Mathematicae*, 35:217–234, 1948.

[3] Gunnar Carlsson. Topological pattern recognition for point cloud data. *Acta Numerica*, 23(1):289–368, 2014.

[4] Gunnar Carlsson and Vin de Silva. Zigzag persistence. *Foundations of Computational Mathematics*, 10:367–405, 2010.

[5] Gunnar Carlsson, Vin de Silva, and Dmitriy Morozov. Zigzag persistent homology and real-valued functions. In *Proceedings of the Twenty-Fifth Annual Symposium on Computational Geometry*, SCG '09, page 247–256, New York, NY, USA, 2009. Association for Computing Machinery.

[6] Michael Charles Crabb and Ioan Mackenzie James. *Fibrewise Homotopy Theory*. Springer London, 1998.

[7] Vin de Silva and Robert Ghrist. Coordinate-free coverage in sensor networks with controlled boundaries via homology. *International Journal of Robotics Research*, 25:1205–1222, 12 2006.

[8] Tamal Krishna Dey and Yusu Wang. *Computational Topology for Data Analysis*. Cambridge University Press, 2022.

[9] Peter Gabriel. Unzerlegbare darstellungen i. *Manuscripta mathematica*, 6:71–104, 1972.

[10] Allen Hatcher. *Algebraic Topology*. Cambridge University Press, 2001.

[11] Sara Kališnik. Alexander duality for parametrized homology. *Homology, Homotopy and Applications*, 15(2):227–243, 2013.

[12] Jean Leray. Sur la forme des espces topologiques et sur les points fixes des representations. *J. Math. Pures Appl.*, 9(24):95–167, 1945.

[13] Steve Y. Oudot. *Persistence Theory: From Quiver Representations to Data Analysis*. Number 209 in Mathematical Surveys and Monographs. American Mathematical Society, 2015.

ETH

Eidgenössische Technische Hochschule Zürich
Swiss Federal Institute of Technology Zurich

Declaration of originality

The signed declaration of originality is a component of every semester paper, Bachelor's thesis, Master's thesis and any other degree paper undertaken during the course of studies, including the respective electronic versions.

Lecturers may also require a declaration of originality for other written papers compiled for their courses.

I hereby confirm that I am the sole author of the written work here enclosed and that I have compiled it in my own words. Parts excepted are corrections of form and content by the supervisor.

Title of work (in block letters):

Evasion Problem – Determining the Existence of Evasion Paths in Mobile Sensor Networks

Authored by (in block letters):

For papers written by groups the names of all authors are required.

Name(s):	**First name(s):**
Sollberger	Julia

With my signature I confirm that

- I have committed none of the forms of plagiarism described in the 'Citation etiquette' information sheet.
- I have documented all methods, data and processes truthfully.
- I have not manipulated any data.
- I have mentioned all persons who were significant facilitators of the work.

I am aware that the work may be screened electronically for plagiarism.

Place, date	**Signature(s)**
Zürich, 14.07.2023	J Sollberger

For papers written by groups the names of all authors are required. Their signatures collectively guarantee the entire content of the written paper.